Realtime Edge Following Using a Wrist-mounted Laser Range Finder

Colin Archibald
Institute for Information Technology
National Research Council
Ottawa, Ontario, Canada K1A 0R6
e-mail: archibald@iit.nrc.ca

Nathalie Colbert
Servo Robot Inc.
1380 Graham Bell
Boucherville, Québec
Canada J4B 6H5

Abstract

A new approach for following an edge with a robotic manipulator is presented. A laser range finder mounted on the wrist of a six degree-of-freedom PUMA robot is used to provide feedback information to servo the robot end-effector. The objective is to maintain a constant position and orientation of the end effector with respect to the edge being tracked. The laser range finder and the realtime robot controller are described briefly. The method of controlling the path of the robot end effector using the range data in the control loop is presented in detail. An accuracy fixture used to analyze the performance of the edge following was machined from a large block of aluminum. Paths that simulate weld seams were machined into this fixture. An exact geometric model of the seam and the surface of the fixture are used to determine the accuracy of the robot end effector as it follows the path. Uses of this visual servoing method for welding, edge finishing, flame cutting, and application of adhesives are proposed.

1 Introduction

The development of inexpensive, powerful microprocessors and reliable sensors has created the opportunity to increase the capabilities of robotic manipulators. Significant unsolved problems lie in the area of creating intelligent, or at least responsive, behaviours for the robots using these new technologies. One step in this direction is the development of a computing system that allows the sensor data to be used in the control loop of the robot. *Sensor-based* control is required to perform responsive realtime skills, such as edge following.

Robotic edge following is a behaviour that can be described briefly as maintaining the end effector of a manipulator in a constant position and orientation (pose) with respect to an edge on a surface while accommodating variations in the geometry of the surface and the edge itself. Nayak and Ray [1, 2] addressed this problem by using a model-based approach with interesting methods for weld seam identification and following. They used a fixed control cycle of alternating the collection and interpretation of sensor data followed by moving the robot. The methods presented here are significantly different from those of Nayak and Ray in the sensing, control architecture, and in the method of tracking the edge using relative motion as opposed to correcting the position of the end effector in the *world*, or any fixed, coordinate system.

An experimental apparatus has been constructed to test the methods described. A laser range finder developed at the National Research Council [3] is used to provide the geometric data containing the edge and adjacent surface. This is an active sensor which projects a spot of laser light that is scanned across a surface measuring the range by triangulation. This type of sensory feedback provides fast and accurate range data from the perspective of the end effector and has been used to create many interesting behaviours for robotic manipulators for experimental and industrial purposes [4, 5, 6].

The algorithms developed for realtime edge following can be applied in many industrial applications, including seam welding, edge finishing, and application of adhesives.

Section 2 of this paper contains a brief description of the experimental apparatus, including the range finder and the computing architecture. Section 3 covers the algorithm that was developed for the edge following operation. The accuracy fixture machined from a block of aluminum and the use of this fixture

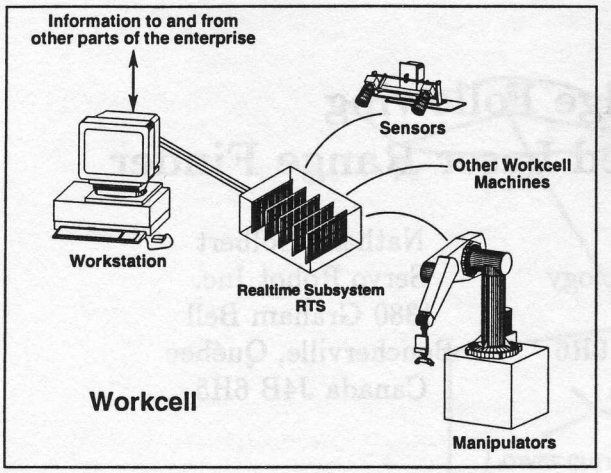

Figure 1: A general view of the system architecture of the workcell.

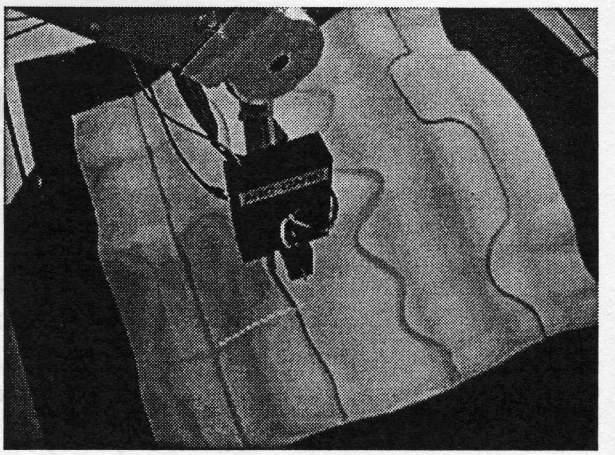

Figure 2: The rangefinder mounted on the PUMA wrist during an edge following experiment.

to analyze the performance of the edge following are in Section 4. Conclusions are in Section 5.

2 Apparatus

The apparatus used in these experiments follows our general concept of the manufacturing workcell, which contains a workstation, a realtime subsystem (RTS), and various sensors, manipulators, and other workcell machines, such as conveyors and parts feeders. A diagram of the workcell design is shown in Figure 1. The workstation is used to interface the workcell to the human programmer or operator and to communicate with the rest of the enterprise. The RTS does most of the computation, collecting data from the sensors, making decisions for the controllable machines, and either controlling the machines directly or sending commands to the other computers that serve as machine controllers. Only one manipulator and one sensor are used in this experiment. The manipulator is a PUMA 560 robot, which is controlled in continuous path mode by communicating to the controller through the Alter port. This method of path control requires that the RTS provide data to the controller every 28 ms. The sensor is a laser range finder mounted on the wrist of the PUMA.

2.1 Laser Range Finder

There are several advantages to using active range finding devices as opposed to passive optical sensors that use ambient or external light sources. Most important, these range finders are capable of providing accurate and explicit 3-D information relative to the end effector of a robot. Because the range data is compact, interpretation can be accomplished in real time without special-purpose image processing hardware. The range finder developed at NRC is specifically designed to be attached to the robot wrist, and the one used in this experiment has a depth of view from approximately 10 cm to 100 cm, with 40° of scanning in the Y direction. Figure 2 shows the rangefinder mounted on the wrist of the PUMA 560 robot during an edge-following experiment.

Physically the sensor must be compact for use on a light payload industrial robot. The prototype sensor has the following physical characteristics: 90 mm width, 140 mm length, 20 mm depth (the depth increases to 80 mm where the galvanometer protrudes), and 500 g in weight including the case. The sensor collects one range profile every 76 ms. The range data collected must be calibrated for use in Cartesian space [8].

The accuracy of the rangefinder is dependent on the optical configuration that defines the field of view. With a 1 m depth of view, the accuracy has been determined in the Z dimension by collecting range data in ideal conditions on a calibration bench. The errors are consistently measured at ± 0.1 mm at standoffs less than 15 cm, and ± 0.2 mm at a standoff of 25 cm, ± 2.0 mm at a standoff of 85 cm, and deteriorate rapidly to about ± 20 mm at a standoff of 100 cm.

2.2 The Computing Architecture

The experimental architecture called SKORP - SKills-Oriented Robot Programming [9] was used in these experiments. The SKORP architecture is de-

signed across two very different machines to provide both the realtime programmer and the application programmer with a suitable environment. The application programmer's workstation is implemented on a Macintosh computer, and the realtime subsystem uses the Harmony operating system [10] with four MC68020 processors. In this hybrid computing environment, the robot operation is created on the workstation, invoking skills that are implemented on the RTS.

The RTS is an object-based system. Besides skills, the major objects in the RTS are Logical Sensors [11], Sensor Drivers, and Machine Controllers. Each of these objects is reusable by other skills and is invoked and communicate by receiving and sending messages. This message passing paradigm guarantees consistent use of the software objects and provides data encapsulation [12].

3 The Edge-following Algorithm

The ultimate objective is to have the robot end effector move in the X direction of the end effector coordinate system at a constant speed while maintaining a constant pose of the end effector relative to the edge. For this experiment the objective has been simplified by making the position of the end effector the same as the location where the range finder is currently looking at the edge. The simplification is that the transformation between the range finder and the end effector is not required. The other obvious difference between this experiment and the implementation of this method for applications is that there is no *look ahead* on the edge. In application the range finder is several centimetres ahead of the end effector, which allows the adjustments in the position of the end effector to be based on what has already been seen. Assuming that the range finder to end effector transformation is accurate, the position of the tool can be made more accurate based on the look ahead and trajectory smoothing than can be achieved in this experiment where look ahead is not used. This is demonstrated in Section 4.

The target position of the end effector (in this case the range finder) relative to the edge is expressed as

$$T = \{T_X, T_Y, T_Z, T_{R_X}, T_{R_Y}, T_{R_Z}\} \quad (1)$$

where $T_Y, T_Z, T_{R_X}, T_{R_Y}, T_{R_Z}$ are specified explicitly as translations and rotations, and T_X is used to specify the speed of the end effector along the seam

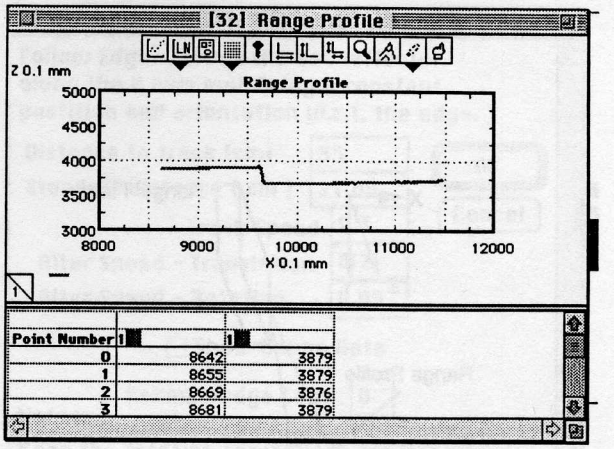

Figure 3: A sample range profile as presented to the programmer.

in the direction of the X axis of the *tool* coordinate system.

The range finder sensor driver collects the range data from a parallel port interface when it is requested by the *Edge-Slope* logical sensor. A sample of the range data containing a step edge of approximately 7 mm is shown in Figure 3. The logical sensor determines the location of the edge by applying a simple one-dimensional differential operator.

The *Follow Edge* skill receives the location of the edge and calculates the amount of correction required in each dimension in the *tool* coordinate system. Since the range data is two dimensional, i.e., Y and Z, the corrections in these degrees of freedom are immediately available:

$$C_Y = T_Y - E_Y \quad (2)$$

$$C_Z = T_Z - E_Z \quad (3)$$

where C_Y and C_Z are the required corrections in the Y and Z directions, and E_Y and E_Z are the detected locations of the edge in Y and Z with respect to the end effector. These corrections are illustrated in Figures 4 and 5.

The correction in rotation around the X axis is also immediately available from calculation of the slope of the surface along the range profile. This slope is calculated as

$$E_{R_X} = \arctan\left(\frac{Z_2 - Z_1}{Y_2 - Y_1}\right) \quad (4)$$

where Z_1, Z_2, Y_1, and Y_2 are two YZ pairs selected from the range profile such that they are both on the same side of the edge. The correction around the X axis is calculated as

$$C_{R_X} = T_{R_X} - E_{R_X} \quad (5)$$

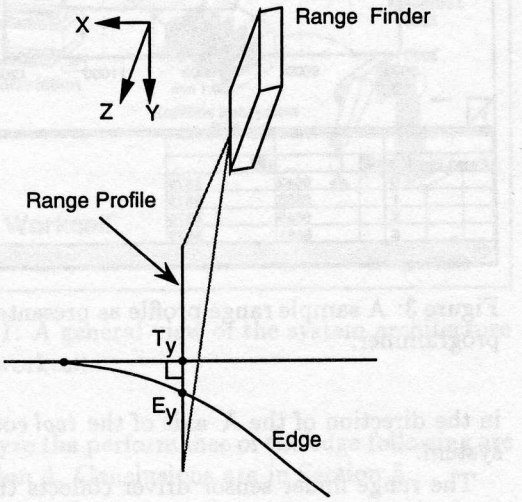

Figure 4: Correction in translation along the end effector's Y axis.

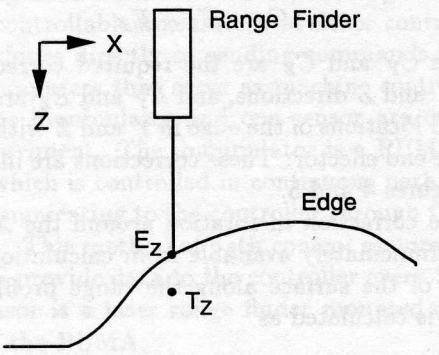

Figure 5: Correction in translation along the end effector's Z axis.

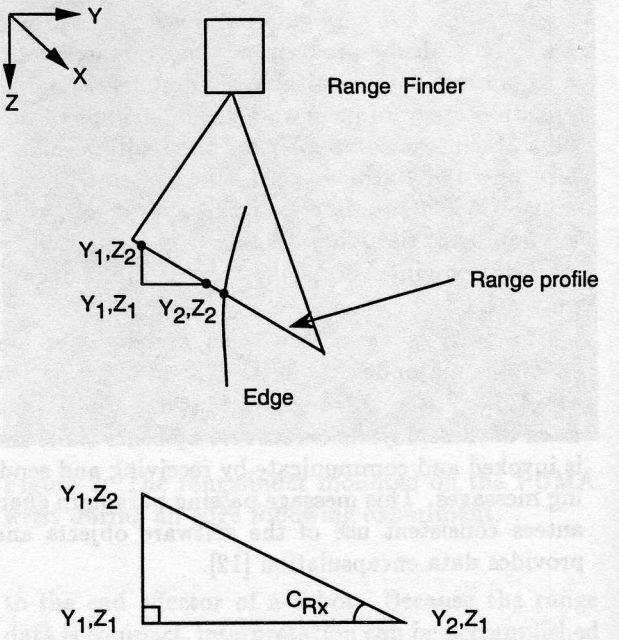

Figure 6: Correction in rotation around the end effector's X axis.

This correction is illustrated in Figure 6.

The corrections around the Y axis, C_{R_Y}, and the Z axis, C_{R_Z}, are calculated based on the sum of recent corrections made in the Y and Z directions. These corrections in translation are stored in a history buffer. The C_Y and C_Z corrections are retained for the last h mm of motion in the X direction, i.e., along the edge. C_{R_Y} and C_{R_Z} are calculated as follows:

$$C_{R_Y} = \arctan\left(\sum C_Z/h\right) \quad (6)$$

$$C_{R_Z} = \arctan\left(\sum C_Y/h\right) \quad (7)$$

where $\sum C_Y$ and $\sum C_Z$ are the total corrections made in the Y and Z directions during the corresponding distance travelled in the X direction, h. These corrections are illustrated in Figures 7 and 8.

Once the corrections are calculated for each degree of freedom, the actual motions sent to the machine controller must be limited to ensure safety and accuracy. Damping functions were not added to the control algorithm in this experiment so that the best possible performance of the sensor/robot combination can be found while facilitating the isolation of sources of error. A damping function, in this case as part of a trajectory filter, has been added in the industrial implementation.

The accuracy criterion is difficult because it depends on three inter-related criteria: the standoff

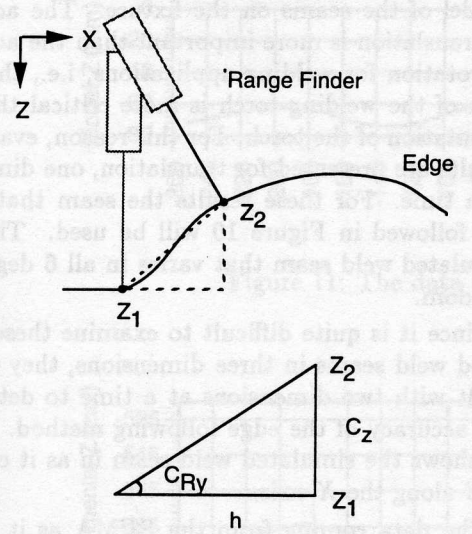

Figure 7: Correction in rotation around the end effector's Y axis.

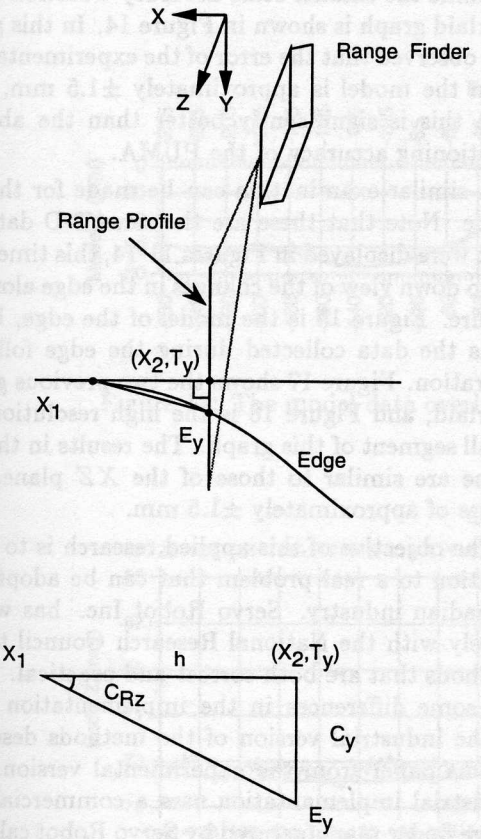

Figure 8: Correction in rotation around the end effector's Z axis.

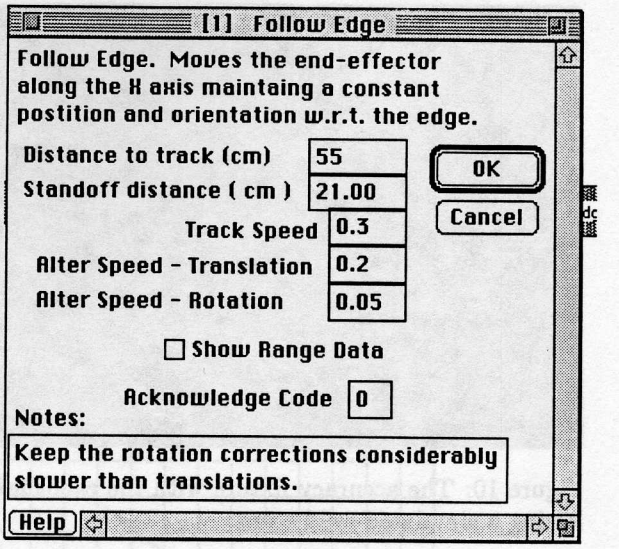

Figure 9: The dialog box used to modify the parameters to the *Follow Edge* skill.

target distance T_Z, the maximum allowable speeds of the corrections in translation and rotation, and the speed of the end effector along the edge.

First, consider the case where the standoff is large. Recall that the accuracy of the range data decreases as the standoff increases. This will reduce the overall accuracy of the system. Combined with this is the speed of the motion along the edge. An increased speed will reduce the accuracy of the edge following, since some time is required to adapt to changes in the edge. This is dependent on the severity of the changes in the edge.

With an exact model of the sensor accuracy, the edge being followed, and the relationships among all control parameters, it may be possible to determine *a priori* parameters for tracking an edge with a known accuracy. This situation is unlikely and unexpected variables, such as position and speed dependent robot dynamics will often invalidate a formal solution. Using the SKORP paradigm, we have created a generic *follow edge* skill with a dialog box that allows the rapid prototyping of a specific edge-following operation. Figure 9 shows the dialog box that was created for this skill. It was found that, for a given standoff and tracking speed, it is quite easy to find a set of parameters for the edge-following operation simply by starting with slow translation and rotation speeds, and observing the behaviour of the end effector as these are gradually increased. Using an interactive dialog box was found to be very helpful in this refinement process. Once it is accepted that a formal solution is not a practical route, the tools for determining an experimentally refined so-

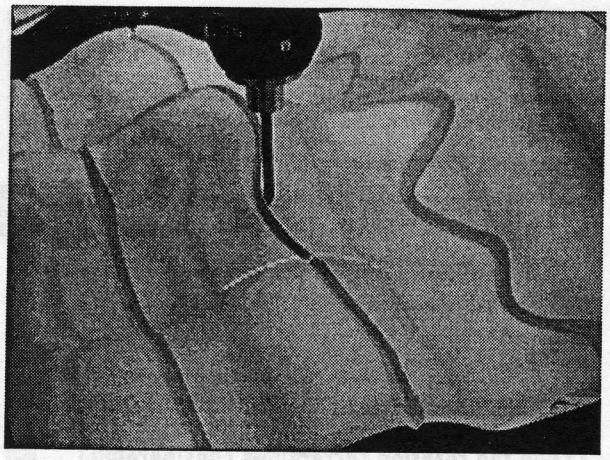

Figure 10: The accuracy fixture with the robot following a simulated weld seam.

lution become critical to the successful application of this method.

4 Evaluation of the System

Visually it is easy to determine that the robot is following the edges and adjusting its pose as the edge changes. Applying the method industrially requires that the performance of the robot be quantified to determine if it can meet the demands of specific applications. This is generally expressed in terms of accuracy and speed, which tend to be traded off against each other. Operations require a high speed while accuracy is not critical or *vice versa*.

It is necessary to have a geometric model of the edge being followed to know if the robot is following accurately. It was determined that a physical model that has an exact geometric model is required to evaluate the performance of the system. An accuracy fixture was machined from a block of aluminum for this purpose. A sculpted surface was created in a CAD package and machined into the aluminum. Simulated weld seams were designed and machined into the sculpted surface. Four seams were created that simulate a relatively easy weld seam, seams of moderate difficulty, and one seam that is believed to contain curves severe enough to represent the most difficult situation that will be encountered. The completed fixture is $61cm \times 61cm \times 15cm$ ($24'' \times 24'' \times 6''$) and can be seen in Figure 10. An accurate geometric representation of the fixture is available from the CAD system that was also used by the NC milling machine.

The evaluation of the system involves collecting data from the robot as it moves along the simulated weld seams and comparing this trajectory with the model of the seams on the fixture. The accuracy in translation is more important than the accuracy in rotation for welding applications, i.e., the position of the welding torch is more critical than the orientation of the torch. For this reason, evaluation results are presented for translation, one dimension at a time. For these results the seam that is being followed in Figure 10 will be used. This is a simulated weld seam that varies in all 6 degrees of freedom.

Since it is quite difficult to examine these simulated weld seams in three dimensions, they will be dealt with two dimensions at a time to determine the accuracy of the edge following method. Figure 11 shows the simulated weld seam in as it changes in Z along the X axis.

The data coming from the PUMA as it travels along the edge is represented similarly. The actual path taken in the XZ plane is shown in Figure 12. These two graphs are overlaid in Figure 13. At this resolution it seems that there is almost no difference between the model and the experimental data. To examine the smaller scale accuracy a section of this overlaid graph is shown in Figure 14. In this graph, it is observed that the error of the experimental data from the model is approximately ± 1.5 mm. Note that this is significantly better than the absolute positioning accuracy of the PUMA.

A similar examination can be made for the XY plane. Note that these are the same 3-D data sets that were displayed in Figures 11-14, this time using a top down view of the changes in the edge along the fixture. Figure 15 is the model of the edge, Figure 16 is the data collected during the edge following operation. Figure 17 shows the two previous graphs overlaid, and Figure 18 is the high resolution of a small segment of this graph. The results in the XY plane are similar to those of the XZ plane, with errors of approximately ± 1.5 mm.

The objective of this applied research is to find a solution to a real problem that can be adopted by Canadian industry. Servo Robot Inc. has worked closely with the National Research Council to find methods that are both correct and practical. There are some differences in the implementation detail of the industrial version of the methods described in this paper from the experimental version. The industrial implemantation uses a commercial laser range finder manufactured by Servo Robot called an M-SPOT 90. This sensor, designed specifically for welding applications, has a 90 mm depth of view. The robot used was manufactured by Panasonic is called the PANA-ROBO AW 010A. This robot is

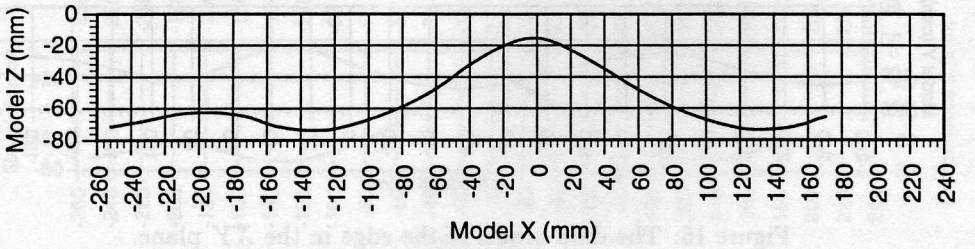

Figure 11: The data model of the edge in the XZ plane.

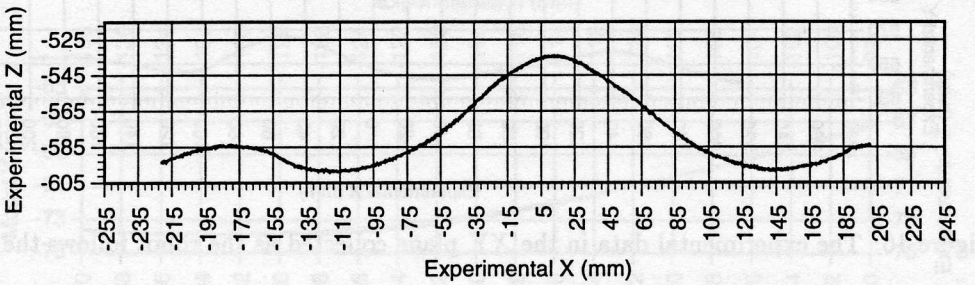

Figure 12: The experimental data in the XZ plane collected as the robot follows the edge.

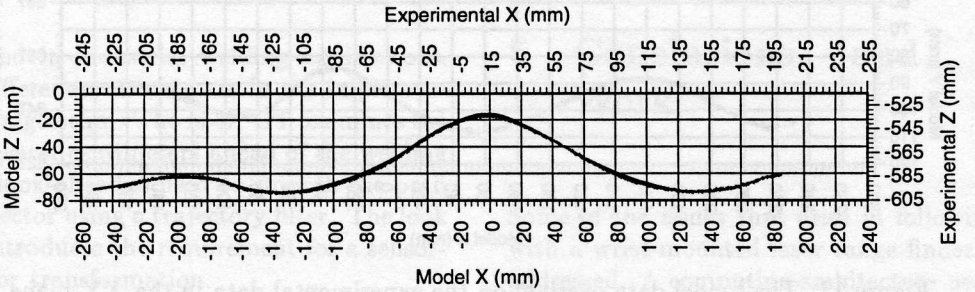

Figure 13: The model data overlaid on the experimental data in the XZ plane.

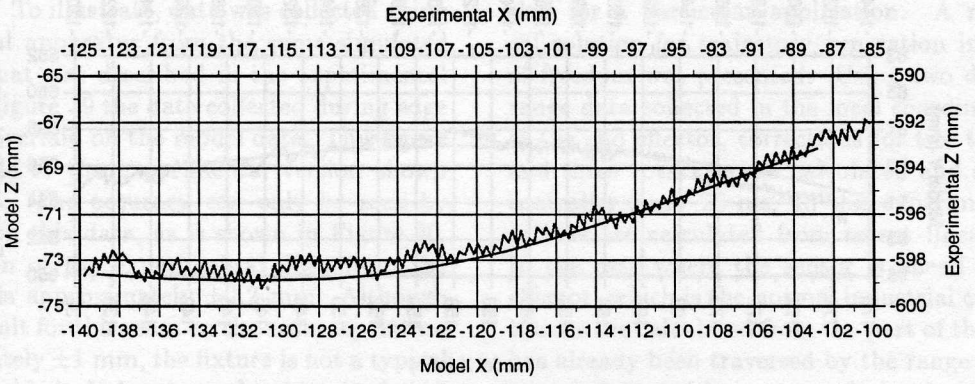

Figure 14: A high resolution section of the data in Figure 13.

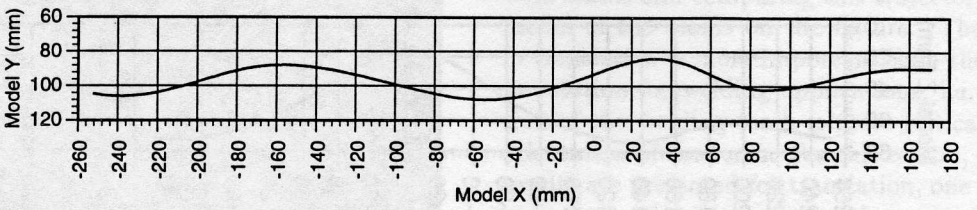

Figure 15: The data model of the edge in the XY plane.

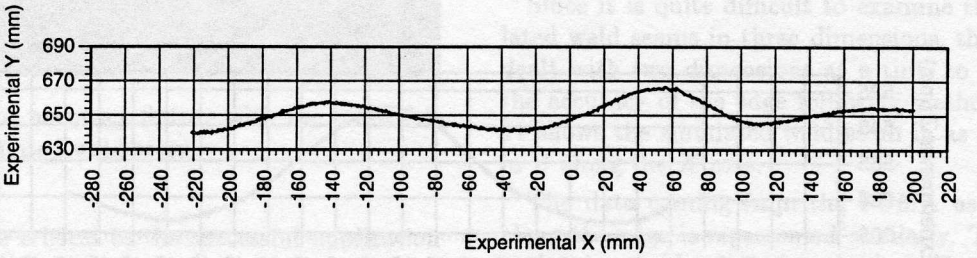

Figure 16: The experimental data in the XY plane collected as the robot follows the edge.

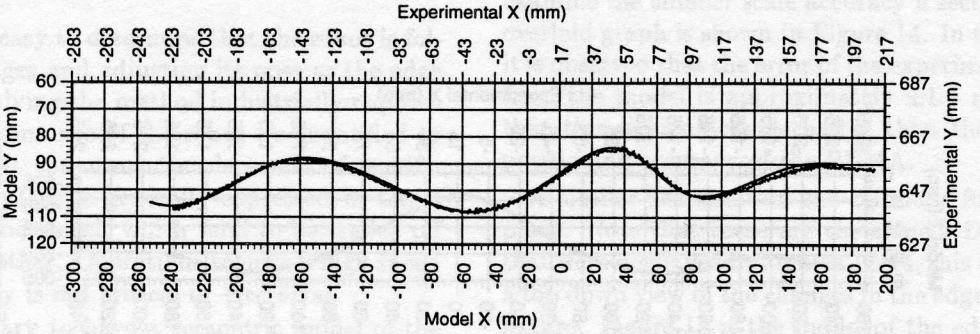

Figure 17: The model data overlaid on the experimental data in the XY plane.

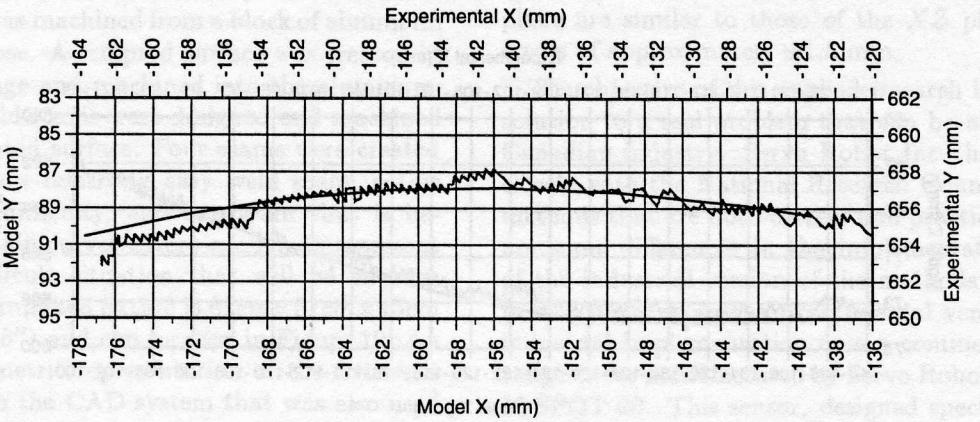

Figure 18: A high resolution section of the data in Figure 17.

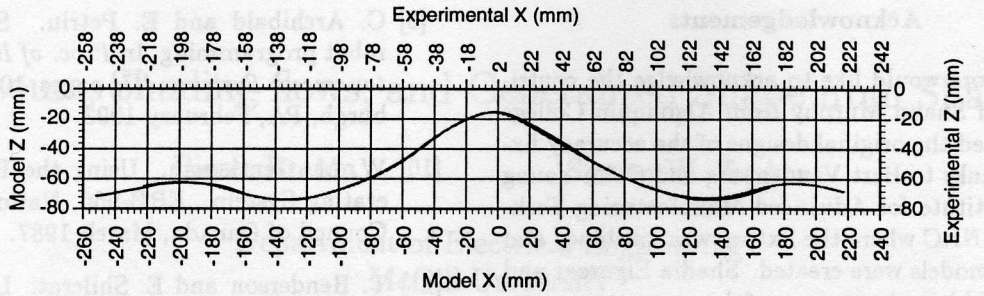

Figure 19: The experimental data overlaid on the model data in the XZ plane, using the commercial sensor and welding robot.

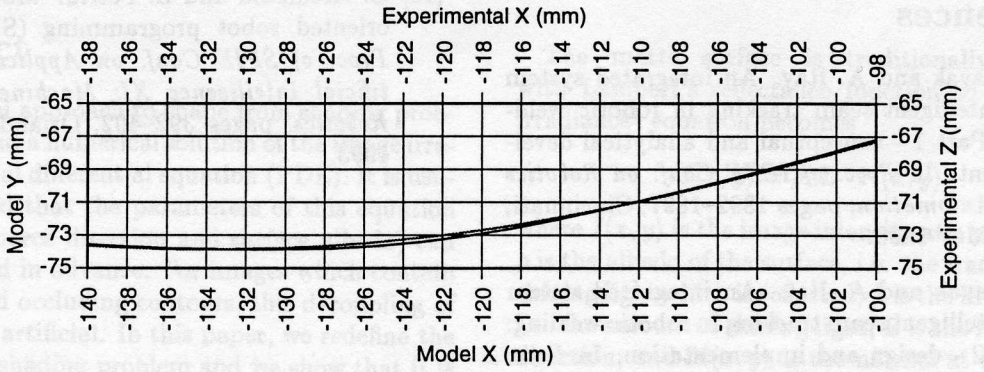

Figure 20: A high resolution section of the data in Figure 19.

widely applied in industrial welding applications. The other differences to note are in the implementation of the algorithm. The M-SPOT examines the weld seam several centimeters ahead of the welding torch. This look-ahead is used to smooth the path of the end effector using a trajectory filter. The look ahead also introduces the requirement for a sensor-to-end effector transformation.

The results of the industrial implementation are encouraging. To illustrate, data was collected using the industrial apparatus from the same simulated weld seam that was described in the experimental version. In Figure 19 the data collected during edge following is overlaid on the model data. This figure is comparable to the experimental version shown in Figure 13. The accuracy can only be seen by zooming in on this data, as is shown in Figure 20. The variation of the experimental data from the model data is approximately ± 0.2 mm. Although the worst result for this seam on the accuracy fixture is approximately ± 1 mm, the fixture is not a typical part to be welded. It has been demonstrated that for parts that are currently being welded by robot, the accuracy varies from ± 0.2 mm to ± 0.4 mm.

5 Conclusions and Future Work

Some of the issues that arise in following an edge with a wrist-mounted laser range finder have been addressed. A computing architecture used for real-time control of a manipulator that uses sensor data in the control loop was described. An experimental system using interactive dialog boxes was used to quickly determine the required parameters of the skill for a particular application. A mathematical solution for trajectory generation in 6 degrees of freedom was presented. Using two dimensional range data collected in the local coordinate system of the end effector, corrections for two translations and three rotations are calculated and sent to the controller every 28 ms. In this experiment the rotations are calculated from recent linear motions. In the case where the sensor is ahead of the end effector, which is the normal industrial case, the rotations are calculated from the part of the edge that has already been traversed by the range finder. Using a robot and laser range finder designed specifically for welding tasks accuracies of ± 0.2 to ± 1.0 mm have been achieved.

Acknowledgements

The authors would like to acknowledge the contributions of Shaun Murphy from Algonquin College who created the original designs of the accuracy fixture. Thanks to Bert Vandenberg and Colin Young of the Institute for Advanced Manufacturing Technology at NRC where the fixture was machined and the data models were created. Shadia Elgazzar and Evelyn Kidd made many useful comments on previous drafts of this work.

References

[1] N. Nayak and A. Ray. An integrated system for intelligent seam tracking in robotic welding: Part 1 - conceptual and analytical development. In *Proc. of IEEE Conf. on Robotics and Automation*, pages 1892–1897, Cincinnati, OH, May 1990.

[2] N. Nayak and A. Ray. An integrated ststem for intelligent seam tracking in robotic welding: Part 2 - design and implementation. In *Proc. of IEEE Conf. on Robotics and Automation*, pages 1898–1903, Cincinnati, OH, May 1990.

[3] M. Rioux, G. Bechthold, M. Duggan, and D. Taylor. Design of a large depth of view 3-D camera for robot vision. *Optical Engineering*, 26(12):1245–1250, December 1987.

[4] S. Venkatesan and C. Archibald. Use of wrist-mounted range profile sensors for real-time tracking. *J. of Machine Vision and Applications*, 5:1–16, 1992.

[5] G. Roth, D. O'Hara, and M. D. Levine. A holdsite method for parts acquisition using a laser rangefinder mounted on a robot wrist. *J. Robotic Systems*, 6(5):573–599, 1989.

[6] C. Archibald and M. van de Panne. Tracking and grasping moving objects using reflex behaviour. In *Proc. of 5th Int'l Conf. on Advanced Robotics (ICAR)*, pages 643–648, Pisa, Italy, June 1991.

[7] M. Rioux. Laser range finder based on a synchronized scanner. *Appl. Opt.*, 23(21):3837–3844, 1984.

[8] S. Amid, B. Trethewey, and C. Archibald. A System for Calibrating the Wrist-mounted Laser Range Finder. ERB-1012, National Reseearch Council of Canada, November 1988.

[9] C. Archibald and E. Petriu. Skills-oriented robot programming. In *Proc. of Intelligent Autonomous Systems III*, pages 104–113, Pittsburgh, PA, February 1993.

[10] W. M. Gentleman. Using the Harmony Operating System. ERB-966, National Research Council of Canada, March 1987.

[11] T. Henderson and E. Shilcrat. Logical sensor systems. *J. of Robotic Systems*, 1(2):169–193, 1984.

[12] C. Archibald and E. Petriu. Model for skills-oriented robot programming (SKORP). In *Proc. of SPIE Conf. on Applications of Artificial Intelligence XI: Machine Vision and Robotics*, pages 392–402, Orlando, FL, April 1993.